CONF-8511126--1

To be published in the proceedings of the International Symposium on Flux Pinning and Electromagnetic Properties in Superconductors, Fukuoka, Japan, November 11-14, 1985.

CONF-8511126--1

DE86 003090

FLUX-LINE PINNING BY THE GRAIN BOUNDARY IN NIOBIUM BICRYSTALS

H. R. Kerchner, D. K. Christen, E. M. Lee, and A. DasGupta

Oak Ridge National Laboratory
Oak Ridge, Tennessee

B. C. Cai and Y. T. Chou

Lehigh University
Bethlehem, Pennsylvania

MASTER

SOLID STATE DIVISION
OAK RIDGE NATIONAL LABORATORY
Operated by
MARTIN MARIETTA ENERGY SYSTEMS, INC.
for the
UNITED STATES DEPARTMENT OF ENERGY
Oak Ridge, Tennessee

November 1985

FLUX-LINE PINNING BY THE GRAIN BOUNDARY IN NIOBIUM BICRYSTALS

H. R. Kerchner,* D. K. Christen,* E. M. Lee,* and A. DasGupta*
Oak Ridge National Laboratory
P. O. Box X, Oak Ridge, Tennessee, USA, 37831

B. C. Cait and Y. T. Chou†
Department of Metallurgy and Materials Engineering, Lehigh University
Bethlehem, Pennsylvania, USA, 18015

Flux-line pinning by the grain boundary in niobium bicrystals was investigated by making four-terminal measurements of the critical current and neutron diffraction measurements of the flux-line bending. The elementary pinning interaction is estimated from the critical current data by using an approximate theory of the current distribution on the grain boundary. The data reported here are mainly for a sample in which the applied magnetic field is parallel to the [111] and the [001] crystal directions in the two grains when it is in the plane of the boundary and perpendicular to the current direction. Evidence is seen of grain boundary faceting and of a flux-flow rectification effect that peaks as a function of temperature below 3 K. The scale of the grain-boundary pinning is consistent with the quasiparticle-scattering theory.

The development of procedures for growing niobium bicrystals$^{1)}$ affords investigations of flux-line (FL) pinning by individual grain boundaries (GB). Although the statistical-summation problem is eliminated, such investigations give no simple measure of the fundamental pinning interaction because an extended defect, such as a GB, is itself a complex entity. Most previous studies of pinning by extended defects have not dealt adequately with this complexity. In the present work we address the related issues of field alignment with the GB, current-induced FL bending, and pinning interaction area by combining four-terminal electrical measurements, small-angle neutron-scattering (SANS) measurements, and a theoretical analysis of the current distribution over the GB. We focus on the most interesting sample although most conclusions apply to all the bicrystals, whose characteristics are summarized and compared elsewhere here in these proceedings.$^{2)}$

The sample is cylindrical, about 3 mm in diameter in the 10-mm gauge length (but of larger diameter where current is injected at the ends), and the GB splits the sample longitudinally through its axis as indicated in Fig. 1. Also shown in Fig. 1 are the orientations of the two grains and the directions of the applied magnetic field H and the applied current I in the positive sense in the convention of this paper. For positive H and I the FL feel a driving force pointing left, from the [001] grain toward the [111] grain. The closed circles indicate the isosceles ([001] grain) and equilateral ([111] grain) triangular FL lattices (FLL) observed in this sample by SANS.

Measurements were made with the applied field H oriented parallel to the GB as shown in Fig. 1 or rotated a small angle Γ from the GB. The neutron scattering measurements were made at the 30-m SANS facility at Oak Ridge with H and the neutron beam both horizontal. The sample and H were rotated together about the vertical sample axis through the rocking angle ϕ in order to investigate the FL curvature at various

---

*Research sponsored by the Division of Materials Sciences, U.S. Department of Energy under contract DE-AC05-84OR21400 with Martin Marietta Energy Systems, Inc. †Research sponsored by the National Science Foundation under Grant DMR79-15799.

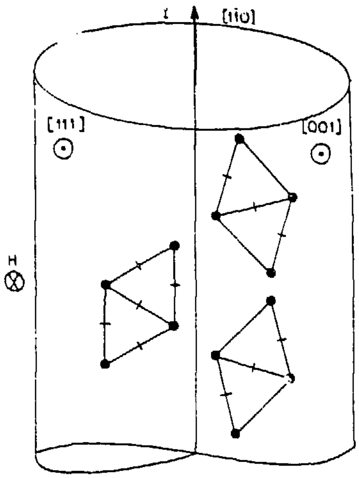

Fig. 1 Schematic illustration of bicrystal showing the orientation of the two grains, the directions of positive H and I, and the observed FLL (solid circles) at 4.8 K.

levels of applied current I. For investigating the critical current a constant current larger than the critical value was applied and the dc flux-flow voltage was measured as H was rotated through the angle Γ.

In order to begin an interpretation of the neutron rocking curves, we present here a simple model of the FL curvature neglecting the pinning effects of the GB. We assume uniform I and H oriented as in Fig. 1. This produces the flux density

$$B = B_0 + I \times B_0 z/2a^2H, \qquad (1)$$

and implies the neutron scattering intensity,

$$I(\phi) = I(0)[1 - (2\pi aH/I)^2\phi^2]^{1/2}. \qquad (2)$$

where B_0 is the equilibrium flux density at the applied field H, a is the sample radius, and z is the spatial coordinate in the direction of H measured from the sample axis.

In spite of the simplicity of this model, the experimental rocking curves have this shape, and their widths increase with I in accord with Eq. (2) as shown in Fig. 2.

Pinning by the GB plays a secondary role in the SANS measurements but is central to the critical current studies. We present here a simple model of the lossless, surface-current distribution over the GB. In order for FL to interact with the GB over a significant length L they must lie within the interaction distance (i.e., coherence length) $\xi \ll L$ of the boundary. We approximate this requirement by assuming that the local field lies exactly parallel to the GB over the length $L \leq 2a$. In the presence of a uniform current I_u, the surface-current density on the boundary J_b must satisfy

$$\frac{1}{2\pi}\int_{-L/2}^{L/2} \frac{J_b(z')}{z-z'}\,dz' + \frac{I_u z}{2\pi a^2} + \Gamma H = 0 \qquad (3)$$

along with the limit $J_b \leq J_c$, the critical value of J_b, everywhere. The solution of Eq. (3),

$$J_b = [1-(2z/L)^2]^{-1/2}[4\Gamma Hz/L + 4I_u z^2/\pi a^2 L + J_0], \qquad (4)$$

diverges at $|z| = L/2$. Setting the unknown parameter J_0 equal to $2J_c\sqrt{\lambda/L}$ limits $J_b \leq J_c$ in the range $|z| \leq (L/2-\lambda)$. The surface current J_b is assumed to peak smoothly a penetration depth λ short of each end of the length L. The total current carried on the boundary is then

$$I_b = \pi\sqrt{\lambda/L}\,J_c L - I_u L^2/4a^2 - \pi|\Gamma|HL \qquad (5)$$

Finally we choose L so as to maximize I_b giving, in three limits:

$$I_b = 2a(J_c' - |\Gamma|H) - I_u, \text{ for } I_u < I_b, \qquad (6a)$$

$$= \frac{3}{4}\left(\frac{4a^4 J_c'^4}{I_u}\right)^{1/3}, \text{ for } I_u \gg I_b,\ \Gamma = 0, \qquad (6b)$$

$$= aJ_c'^2/2\pi\Gamma H, \text{ for } \Gamma H \gg J_c', \qquad (6c)$$

where the maximum average surface current density $J_c' = \pi J_c\sqrt{\lambda/2a}$ is smaller than the critical value J_c by the factor $\pi\sqrt{\lambda/2a} \simeq .01$ for our sample.

The behavior predicted by the above models is seen in the experimental results along with certain discrepancies that we believe manifest distortions of the GB from ideal planarity. The straight-line fits to the $\Delta\phi$ data (Fig. 2) have the slope given by Eq. 2. However, $\Delta\phi$ fails to approach zero at $I = 0$; indeed, it appears that the FL should be straightest for $I \simeq -4$ A. The larger critical current for $I > 0$ also suggests that positive I tends to match the associated FL curvature to the GB better than $I = 0$.

Details of the four-terminal electrical measurements are shown in Fig. 3. In the lower plot the abscissa is the observed

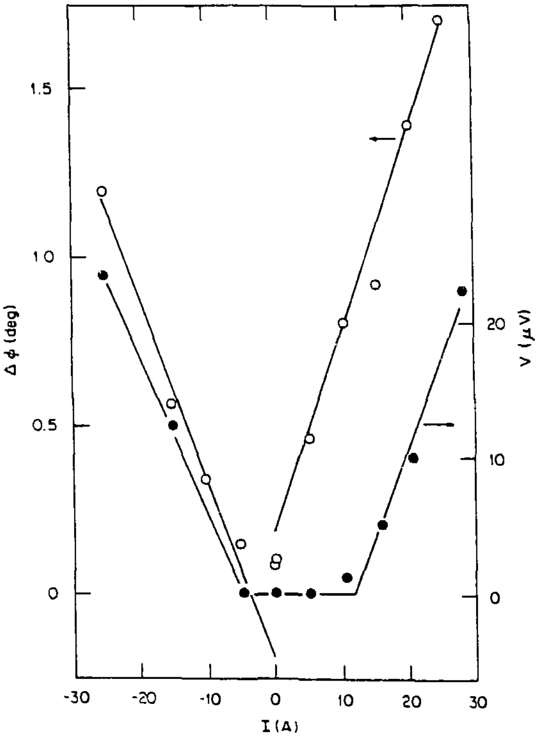

Fig. 2 The full width at half maximum of the SANS rocking curve (open circles) and the flux-flow voltage (solid circles) plotted vs. applied current at $T = 4.8$ K and $B = 0.2$ T.

voltage, divided by the flux-flow resistance and offset by the bulk critical current; that is, it gives the uniform portion I_u of the total applied current I. The ordinate is the angular misalignment between H and the average GB direction. Curves of Γ vs I_u are shown for various total currents I. The difference $I - I_u = I_b$ peaks as a function of Γ with a fine structure that depends on I. The locations (I,Γ) of two dominant contributing peaks are identified by open circles that lie on intersecting straight lines. Near the intersection at $I = 17.5$ A the $I_b(\Gamma)$ peaks are tallest and sharpest, and the angle-integrated values, shown in the upper plot are largest. This behavior suggests that the GB is composed of two flat segments (and some additional smaller segments) misoriented by about 1° (the separation of the intersecting lines at $I = 0$). Similar fine structure observed in another sample changed in detail upon high-temperature degassing. We infer that the apparent segmenting arises from GB pinning by interstitial-gas precipitates.

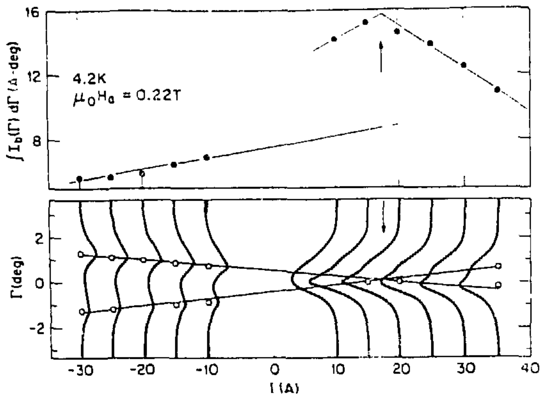

Fig. 3 The angle-integrated GB critical current (upper) and the dips in the uniform bulk current (associated with peaks in the GB current plotted vs. the angle Γ (lower) at 11 applied currents.

The pinning force per unit area of GB $F_b = I_bB/2a$ is summarized in Fig. 4. In spite of fine-structure variations in the $F_b(\Gamma)$ peaks, our data obey simple scaling rules to a reasonable approximation. First, the angle-integrated peaks $\int F_b(\Gamma)d\Gamma$ are nearly the peak values $F_b(\Gamma_p)$ times 2°. Second, $F_b(\Gamma_p)$ has the same dependence on reduced B at all temperatures studied, as shown in Fig. 4b and d. Comparing positive and negative current directions, the B dependences are slightly different, and the temperature dependences show a pronounced disparity. F_{max}^- (corresponding to $I < 0$) increases monotonically with B_{c2}, while the larger F_{max}^+ ($I > 0$) peaks for $B_{c2} \simeq .37$ T, somewhere between 2 and 3 K. Although the difference $F_b^+(\Gamma_p)-F_b^-(\Gamma_p)$ arises in part from the geometrical effect discussed above, we do not ascribe it all to GB distortion because $\int I_b(\Gamma)d\Gamma$, plotted vs. I in Fig. 3, fails to fall on a single smooth curve. Even if the GB were exactly planar, flux-flow rectification would be observed. We believe that this rectification effect must arise from the intrinsic anisotropy of superconducting niobium, although we have no detailed model of its source. The curious temperature dependence of F_{max}^+ and differences in the B dependence of $F_b^+(\Gamma_p)$ and $F_b^-(\Gamma_p)$ suggest that excess pinning of FLL passing from the [001] to the [111] grain may be connected with the FLL structural transition expected

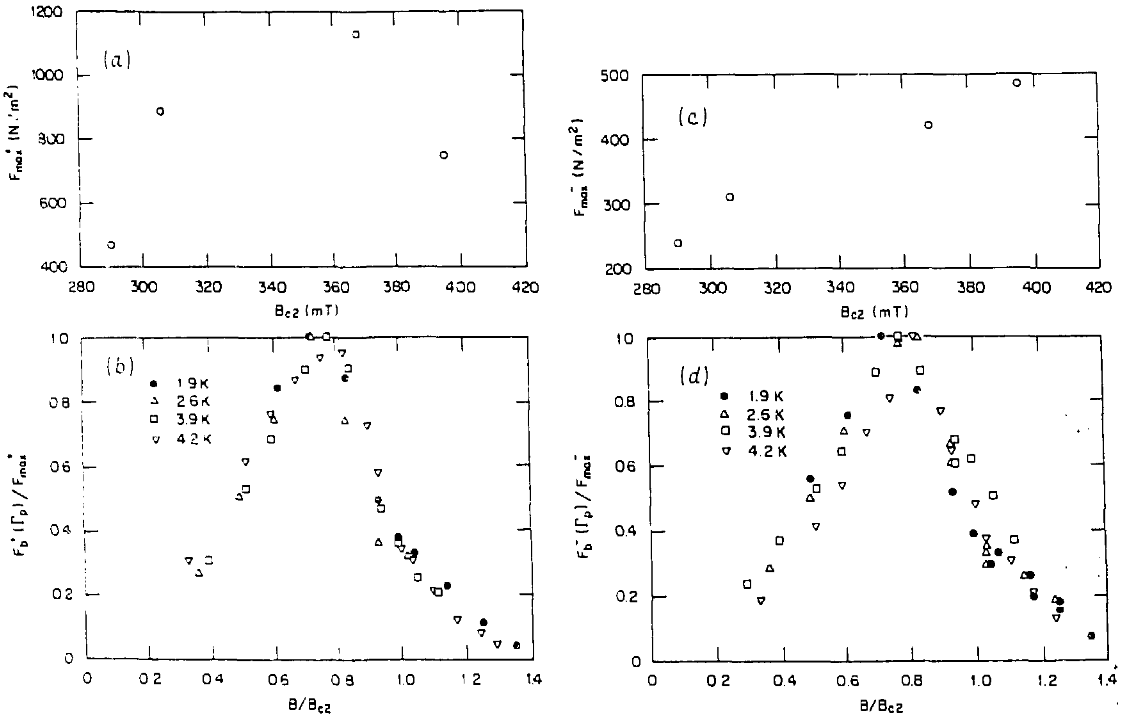

Fig. 4 a. The maximum average pinning force per unit area of GB inhibiting FL motion from the [001] grain into the [111] grain plotted vs. the upper critical flux density B_{c2} at four temperatures. b. The reduced peak value of $F_b(\Gamma)$ plotted vs. reduced flux density B/B_{c2} for the conditions of a. c. Same as a but for FL motion in the opposite direction. d. Same as b but for the FL motion of c.

in the [001] grain near 2 K.[3)]

In order to compare the scale of $F_b(\Gamma_p)$ with a theoretical calculation of the interaction between an infinite, straight FLL and an infinite GB we must multiply the results in Fig. 4 a and c by 100 as explained above. This leads to pinning forces per unit area in the range 10^4 - 10^5 N/m², about equal to the BCS-ground-state condensation energy density $\mu_0 H_c^2$. The theory of FL pinning by the quasiparticle-scattering mechanism[4)] gives an interaction $\delta\Omega \approx \mu_0 H_c^2 \sigma_{tr} \xi_0 |\psi|^2$ with a small scattering center, where ξ_0 is the BCS coherence length, ψ the reduced order parameter, and σ_{tr} the transport cross section of the scatterer. Treating the GB as a planar array of scatterers leads to a maximum pinning force $BJ_c \approx 0.7p\sqrt{b}(1-b)\mu_0 H_c^2$, where p is the product of σ_{tr} and the number of scatterers per unit area of GB. Our observations of both the pinning strength and the nucleation field for local superconductivity on the grain boundary[4)] above B_{c2} consistently require $p \rightarrow 1$.

The theoretical models presented here, combined with the quasiparticle-scattering theory of FL pinning, provide semiquantitative agreement with our observations of GB pinning. A fully quantitative analysis of the experiment is precluded by the lack of detailed knowledge of the microscopic GB structure and by the failure of extant theory to encompass the observed smooth B dependence of J_c through B_{c2}. Future studies of FL pinning by extended defects must deal realistically with the ability of FL to conform to the defect shapes and with the localized superconductivity above B_{c2} on many defect surfaces.

The authors are grateful to S. T. Sekula and F. J. E. Tasset for many helpful discussions and experimental assistance.

---

1) B. C. Cai, A. Das Gupta, and Y. T. Chou, J. Less Common Metals 86, 145 (1982).
2) A. Das Gupta, Y. T. Chou, and B. C. Cai, following paper.
3) D. K. Christen, H. R. Kerchner, S. T. Sekula, and P. Thorel, Phys. Rev. B 21, 102 (1980).
4) E. V. Thuneberg, this volume.